
Decision-Making with Auto-Encoding Variational Bayes

Romain Lopez¹, Pierre Boyeau¹, Nir Yosef^{1,2,3}, Michael I. Jordan^{1,4} and Jeffrey Regier⁵

¹ Department of Electrical Engineering and Computer Sciences,
University of California, Berkeley

² Chan-Zuckerberg Biohub, San Francisco

³ Ragon Institute of MGH, MIT and Harvard

⁴ Department of Statistics, University of California, Berkeley

⁵ Department of Statistics, University of Michigan, Ann Arbor

Abstract

To make decisions based on a model fit by auto-encoding variational Bayes (AEVB), practitioners often let the variational distribution serve as a surrogate for the posterior distribution. This approach yields biased estimates of the expected risk, and therefore poor decisions for two reasons. First, the model fit by AEVB may yield biased statistics relative to the underlying data distribution. Second, there may be strong discrepancies between the variational distribution and the posterior. We explore how fitting the variational distribution based on several objective functions other than the ELBO, while continuing to fit the generative model based on the ELBO, affects the quality of downstream decisions. For the probabilistic principal component analysis model, we investigate how importance sampling error, as well as the biases in model parameter estimates, vary across several approximate posteriors when used as proposal distributions. Our theoretical results suggest that a posterior approximation distinct from the variational distribution should be used for making decisions. Motivated by these theoretical results, we propose learning several approximate proposals for the best model and combining them using multiple importance sampling for decision-making. In addition to toy examples, we present a full-fledged case study of single-cell RNA sequencing. In this challenging instance of multiple hypothesis testing, our proposed approach surpasses the current state of the art. The code and datasets are available at <http://github.com/PierreBoyeau/decision-making-vaes>.

1 Introduction

The auto-encoding variational Bayes (AEVB) algorithm relies on neural networks to amortize approximate inference and performs model selection by maximizing a lower bound on the model evidence [1, 2]. In the specific case of variational autoencoders (VAEs), a low-dimensional representation of data is transformed through a learned nonlinear function (another neural network) into the parameters of a conditional likelihood. VAEs achieve impressive performance on pattern-matching tasks like representation/manifold learning and synthetic image generation [3].

Many machine learning applications, however, require decisions, not just compact representations of the data. Researchers have accordingly attempted to use VAEs for decision-making applications, including novelty detection in control applications [4], mutation-effect prediction from genomic sequences [5], artifact detection [6], and Bayesian hypothesis testing for single-cell RNA sequencing data [7, 8]. To make decisions based on VAEs, these researchers implicitly appeal to Bayesian

decision theory, which counsels taking the action that minimizes expected loss under the posterior distribution [9].

However, for VAEs, the relevant functionals of the posterior cannot be computed exactly. Instead, after fitting a VAE based on the ELBO, practitioners take one of three approaches to decision-making: i) the variational distribution may be used as a surrogate for the posterior [5], ii) the variational distribution may be used as a proposal distribution for importance sampling [10], or iii) the variational distribution can be ignored once the model is fit, and decisions may be based on an iterative sampling method such as MCMC or annealed importance sampling [11]. But will any of these combined procedures (ELBO for model training and one of these methods for approximating posterior expectations) produce good decisions?

They may not, for two reasons. First, estimates of the relevant expectations of the posterior may be biased and/or may have high variance. The former situation is typical when the variational distribution is substituted for the posterior; the latter is common for importance sampling estimators. By using the variational distribution as a proposal distribution, practitioners aim to get unbiased low-variance estimates of posterior expectations. But this approach often fails. The variational distribution recovered by the VAE, which minimizes the reverse Kullback-Leibler (KL) divergence between the variational distribution and the model posterior, is known to systematically underestimate variance [12, 13], making it a poor choice for an importance sampling proposal distribution. Alternative inference procedures have been proposed to address this problem. For example, expectation propagation (EP, [14]) and CHIVI [15] minimize the forward KL divergence and the χ^2 divergence, respectively. Both objectives have favorable properties for fitting a proposal distribution [16, 17]. IWVI [10] seeks to maximize a tight lower bound of the evidence that is based on importance sampling estimates (IWELBO). IWVI empirically improves over VI for estimating posterior expectations. It is unclear, however, which method to choose for a particular application.

Second, even if we can faithfully compute expectations of the model posterior, the model learned by the VAE may not resemble the real data-generating process [13]. Most VAE frameworks rely on the IWELBO, where the variational distribution is used as a proposal [18, 19, 20]. For example, model and inference parameters are jointly learned in the IWAE [18] using the IWELBO. Similarly, the wake-wake (WW) procedure [21, 22] uses the IWELBO for learning the model parameters but seeks to find a variational distribution that minimizes the forward KL divergence. In the remainder of this manuscript, we will use the same name to refer to either the inference procedure or the associated VAE framework (e.g., WW will be used to refer to EP).

To address both of these issues, we propose a simple three-step procedure for making decisions with VAEs. First, we fit a model based on one of several objective functions (e.g., VAE, IWAE, WW or χ -VAE) and select the best model based on some metric (e.g., IWELBO calculated on held-out data with a large numbers of particles). The χ -VAE is a novel variant of the WW algorithm that, for fixed p_θ , minimizes the χ^2 divergence (further details in Appendix B). Second, with the model fixed, we fit several approximate posteriors, based on the same objective functions, as well as annealed importance sampling [11] where applicable. Third, we combine the approximate posteriors as proposal distributions for multiple importance sampling [23] to make decisions that minimize the expected loss under the posterior. In multiple importance sampling, we expect the mixture to be a better proposal than either of its components alone, especially in settings where the posterior is complex because each component helps with different parts of the posterior.

After introducing the necessary background (Section 2), we provide a complete analysis of our framework in setting of the probabilistic PCA model [24] (Section 3). In this tractable setting, we recover the known fact that an underdispersed proposal causes severe error to importance sampling estimators [25]. The analysis also shows that overdispersion may harm the process of model learning by exacerbating existing biases in variational Bayes. We also confirm these results empirically. Next, we perform an extensive empirical evaluation of two real-world decision-making problems. First, we consider a practical instance of classification-based decision theory. In this setting, we show that the vanilla VAE becomes overconfident in its posterior predictive density, which harms performance. We also show that our three-step procedure outperforms IWAE and WW (Section 4). We then present a scientific case study, focusing on an instance of multiple hypothesis testing in single-cell RNA sequencing data. Our approach yields a better calibrated estimate of the expected posterior false discovery rate (FDR) than that computed by the current state-of-the-art method (Section 5).

2 Background

Bayesian decision making [9] makes use of a model and its posterior distribution to make optimal decisions. We bring together several lines of research in an overall Bayesian framework.

2.1 Auto-encoding variational Bayes

Variational autoencoders [1] are based on a hierarchical Bayesian model [26]. Let x be the observed random variables and z the latent variables. To learn a generative model $p_\theta(x, z)$ that maximizes the evidence $\log p_\theta(x)$, variational Bayes [12] uses a proposal distribution $q_\phi(z | x)$ to approximate the posterior $p_\theta(z | x)$. The evidence decomposes as the *evidence lower bound* (ELBO) and the reverse KL variational gap (VG):

$$\log p_\theta(x) = \mathbb{E}_{q_\phi(z|x)} \log \frac{p_\theta(x, z)}{q_\phi(z | x)} + \Delta_{\text{KL}}(q_\phi \parallel p_\theta). \quad (1)$$

Here we adopted the condensed notation $\Delta_{\text{KL}}(q_\phi \parallel p_\theta)$ to refer to the KL divergence between $q_\phi(z | x)$ and $p_\theta(z | x)$. In light of this decomposition, a valid inference procedure involves jointly maximizing the ELBO with respect to the model’s parameters and the variational distribution. The resulting variational distribution minimizes the reverse KL divergence. VAEs parameterize the variational distribution with a neural network. Stochastic gradients of the ELBO with respect to the variational parameters are computed via the reparameterization trick [1].

2.2 Approximation of posterior expectations

Given a model p_θ , an action set \mathcal{A} , and a loss L , the optimal decision $a^*(x)$ for observation x is an expectation taken with respect to the posterior: $\mathcal{Q}(f, x) = \mathbb{E}_{p_\theta(z|x)} f(z)$. Here f depends on the loss [9]. We therefore focus on numerical methods for estimating $\mathcal{Q}(f, x)$. Evaluating these expectations is the aim of Markov chain Monte Carlo, annealed importance sampling (AIS) [27], and variational methods [10].

Although we typically do not have direct access to the posterior $p_\theta(z | x)$, we can, however, sample $(z_i)_{1 \leq i \leq n}$ from the variational distribution $q_\phi(z | x)$. A naive, but practical, approach is to consider a plugin estimator [4, 5, 6, 7]:

$$\hat{\mathcal{Q}}_{\text{P}}^n(f, x) = \frac{1}{n} \sum_{i=1}^n f(z_i), \quad (2)$$

which replaces the exact posterior by sampling z_1, \dots, z_n from $q_\phi(z | x)$. A less naive approach is to use self-normalized importance sampling (SNIS),

$$\hat{\mathcal{Q}}_{\text{IS}}^n(f, x) = \frac{\sum_{i=1}^n w(x, z_i) f(z_i)}{\sum_{j=1}^n w(x, z_j)}, \quad (3)$$

with importance weights $w(x, z) := p_\theta(x, z) / q_\phi(z | x)$. The nonasymptotic behavior of both estimators as well as their variants is well understood [16, 17, 28]. Moreover, each upper bound on the error motivates an alternative inference procedure in which the upper bound is used as a surrogate for the error. For example, [16] bounds on the error of the IS estimator as a function of *forward* KL divergence $\Delta_{\text{KL}}(p_\theta \parallel q_\phi)$, which motivates the WW algorithm in [22]. Similarly, [17] provides an upper bound of the error based on the χ^2 divergence, which in turn justifies our investigation of the χ -VAE. However, these upper bounds are too broad to explicitly compare, for example, the worst-case performance of χ -VAE and WW when f belongs to a function class (further details in Appendix C).

3 Theoretical analysis for pPCA

We aim to understand the theoretical advantages and disadvantages of each objective function used for training VAEs and how they impact downstream decision-making procedures. Because intractability prevents us from deriving sharp constants in general models, to support a precise theoretical analysis, we consider probabilistic principal component analysis (pPCA) [29]. pPCA is a linear model for

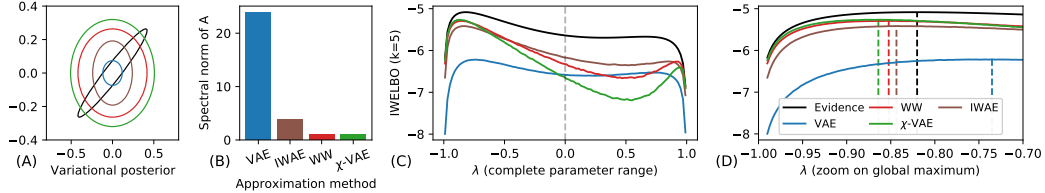


Figure 1: Variational Bayes for the bivariate pPCA example. (A) Gaussian mean-field approximations to the posterior (same legend for all the figures) (B) Corresponding values of $\|A\|_2$ (C) IWELBO ($k = 5$) as a function of λ , with proposals estimated for $\lambda = 0$ and other model parameters fixed to their true values (D) Specific zoom around the global maximum.

which posterior inference is tractable. Though the analysis is a special case, we believe that it provides an intuition for performance of our decision-making procedures more generally because, for many of the models that are used in practice, a Gaussian distribution approximates the posterior well, as demonstrated by the success of the Laplace approximation [30].

In pPCA, the latent variables z generate data x . We use an isotropic Gaussian prior on z and a linear model with spherical Gaussian observation model for x :

$$\begin{aligned} p_\theta(z) &= \text{Normal}(0, I) \\ p_\theta(x | z) &= \text{Normal}(Wz + \mu, \sigma^2 I). \end{aligned} \quad (4)$$

To make model selection challenging, we follow [13] and parameterize $\sigma^2 = 1/(1-\lambda^2)$ as well as $W_{ij} = e^\lambda W'_{ij}$ if $i \neq j$ and $W_{ij} = W'_{ij}$ otherwise. In this setting, $\theta := (W', \mu, \lambda)$. We consider an amortized posterior approximation,

$$q_\phi(z | x) = \text{Normal}(h_\eta(x), D(x)), \quad (5)$$

where h_η is a neural network with parameters η , $D(x)$ is the diagonal covariance matrix given by $\text{diag}(h_\xi(x))$, and h_ξ is a neural network with parameters ξ . In this example, the encoder parameters are $\phi = (\eta, \xi)$.

3.1 Approximate posterior variance

Exploiting the invariance properties of Gaussian distributions [31], our next lemma gives concentration bounds for the logarithm of the importance sampling weights under the posterior.

Lemma 1. (Concentration of the log-likelihood ratio) *For an observation x , let Σ be the variance of the posterior distribution under the pPCA model, $p_\theta(z | x)$. Let*

$$A(x) = \Sigma^{1/2} [D(x)]^{-1} \Sigma^{1/2} - I. \quad (6)$$

For z following the posterior distribution, $\log w(x, z)$ is a sub-exponential random variable. Further, there exists a $t^(x)$ such that, under the posterior $p_\theta(z | x)$ and for all $t > t^*(x)$,*

$$\mathbb{P}(|\log w(x, z) - \Delta_{KL}(p_\theta \| q_\phi)| \geq t) \leq e^{-\frac{t}{8\|A(x)\|_2}}. \quad (7)$$

This lemma characterizes the concentration of the log-likelihood ratio, a central quantity to all the VAE variants we analyze, as the spectral norm of a simple matrix $\|A(x)\|_2$. Plugging the concentration bound from Lemma 1 into the result of [16], we obtain an error bound on the IS estimator for posterior expectations.

Theorem 1. (Sufficient sample size) *For an observation x , suppose that the second moment of $f(z)$ under the posterior is bounded by κ . If the number of importance sampling particles n satisfies $n = \beta \exp\{\Delta_{KL}(p_\theta \| q_\phi)\}$ for some $\beta > \log t^*(x)$, then*

$$\mathbb{P}\left(|\hat{\mathcal{Q}}_{IS}^n(f, x) - \mathcal{Q}(f, x)| \geq \frac{2\sqrt{3\kappa}}{\beta^{1/8\gamma} - \sqrt{3}}\right) \leq \frac{\sqrt{3}}{\beta^{1/8\gamma}}, \quad (8)$$

with $\gamma = \max(1, 4\|A(x)\|_2)$

Table 1: Results on the pPCA simulated data. MAE refers to the mean absolute error in posterior expectation estimation.

	VAE	IWAE	WW	χ -VAE
$\log p_\theta(X)$	-17.65	-16.91	-16.93	-16.92
IWELBO	-17.66	-16.92	-16.96	-16.92
$\ A\ _2$	1.69	1.30	2.32	1.13
PSIS	0.54	0.53	0.66	0.47
MAE	0.103	0.032	0.043	0.030

Theorem 1 identifies a key quantity—the spectral norm of $A(x)$ —as useful for controlling the sample efficiency of the IS estimator. Interestingly, the closed-form expression for $\|A(x)\|_2$ from Eq. (6) suggests overestimating the posterior variance is often more suitable than underestimating variance. For the one-dimensional problem, $\|A(x)\|_2$ is indeed asymmetric around its global minimum, favoring larger values of $D(x)$.

As a consequence of this result, we can characterize the behavior of several variational inference frameworks such as WW, χ -VAE, IWAE, and VAE (in this case, the model is fixed). We provide this analysis for a bivariate Gaussian example in which all the quantities of interest can be visualized (full derivations in Appendix D). Figure 1A shows that the VAE underestimates the variance while other frameworks provide adequate coverage of the posterior. As expected, $\|A\|_2$ is significantly smaller for WW and the χ -VAE than for the VAE (Figure 1B).

3.2 Model selection

In the VAE framework, the model parameters must also be learned. For a fixed variational distribution, variational Bayes (VB) selects the model that maximizes the ELBO or the IWELBO. Each approximate posterior inference method proposes a different lower bound. Even though all these lower bounds become tight (equal to the evidence) with an infinite number of particles, the different proposal distribution might not perform equally for model selection because a finite number of particles is used in practice. Moreover, because the optimal IS proposal depends on the target function [32], a good proposal for model learning may not be desirable for decision-making and vice versa.

We can further refine this statement in the regime with few particles. VB estimates of the model parameters are expected to be biased towards the regions where the variational bound is tighter [13]. For a single particle, the tightness of the IWELBO (hence equal to the ELBO) is measured by the reverse KL divergence:

$$\Delta_{\text{KL}}(q_\phi \parallel p_\theta) = \frac{1}{2} \left[\text{Tr} [\Sigma(\theta)^{-1} D(x)] + \log \det \Sigma(\theta) \right] + C, \quad (9)$$

where C is constant with respect to θ . Interestingly, because $\Delta_{\text{KL}}(p_\theta \parallel q_\phi)$ is linear in $D(x)$, a higher variance $D(x)$ in Eq. (9) induces a higher sensitivity of variational Bayes in parameter space. For multiple particles, no closed-form solution is available so we proceed to numerical experiments on the bivariate pPCA example. We choose five particles. In this setting, the approximate posteriors are fit for an initial value of the parameter $\lambda = 0$ (the real value is $\lambda = 0.82$) with all other parameters set to their true value. WW and the χ -VAE exhibit in Figure 1C a higher sensitivity than the VAE and the IWAE, similarly to the case with a single particle. This sensitivity translates into higher bias for selection of λ (Figure 1D). These results suggest that lower variance proposals may be more suitable for model learning than for decision-making, providing yet another motivation for using different proposals for each task.

3.3 Experimental results

We now investigate the behavior of WW, the χ -VAE, IWAE, and the VAE for the same model, but in a higher-dimensional setting. In particular, we generate synthetic data according to the pPCA model described in Eq. (4) and assess how well these variants can estimate posterior expectations.

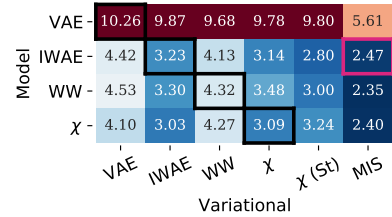


Figure 2: MAE ($\times 10^2$) of posterior expectation estimation on pPCA for combinations of VAEs (row) and inference only (columns) frameworks.

Our complete experimental setup is described in Appendix E. We use a linear function for the mean and the log-variance of the variational distribution. This is a popular setup for approximate inference diagnostics [13] since the posterior has an analytic form, and the form is not typically a mean-field factorization. We propose a toy example of a posterior expectation, $\mathcal{Q}(f_\nu, x) = p_\theta(z_1 \geq \nu \mid x)$, obtained for $f_\nu(z) = \mathbb{1}\{e_1^\top z \geq \nu\}$ with e_1 as the first vector of the canonical basis of \mathbb{R}^d . For this choice of f_ν , the resulting posterior expectation is tractable since it is the cumulative density function of a Gaussian distribution.

To evaluate the learned generative model, we provide goodness-of-fit metrics based on IWELBO on held-out data as well as the exact log-likelihood. In addition, we report the Pareto-smoothed importance sampling (PSIS) diagnostic k for assessing the quality of the variational distribution as a proposal [25]. PSIS is computed by fitting a generalized Pareto distribution to the IS weights; it indicates the viability of the variational distribution for IS. For multiple importance sampling (MIS), we combine the proposal (learned on the same model) from IWAE, WW, and χ -VAE, as well as samples from the prior [33] with equal weights.

When not stated otherwise, we report the median PSIS over 64 observations, using 5,000 samples from the posterior. Unless stated otherwise, we use 30 particles (also for the VAE, as in [19]) per iteration for training the models, 10,000 samples for reporting log-likelihood proxies and 200 particles for making decisions. All results are averaged across five random initializations of the neural network weights.

Table 1 contains our results for 5 particles for the pPCA model. IWAE, WW, and the χ -VAE outperform the VAE in terms of held-out exact likelihood (always close to the IWELBO). There is a slight preference for IWAE. In terms of posterior approximation, we find that all algorithms yield a reasonable value for the PSIS diagnostic, in overall agreement with the spectral norm of A . PSIS values are not directly comparable between models, as they only measure the suitability of the variational distribution for a particular model. Results for more particles can be found in the annex. Finally, in terms of mean absolute error (MAE), IWAE and χ -VAE achieve the best result. For the VAE, the plugin estimator attains similar performance as the SNIS estimator.

In Figure 2, we fix these models and learn several proposal distributions for estimating the posterior expectations. For a fixed model, the proposal from the χ -VAE often improves the MAE, and the one from MIS performs best. The three-step procedure (IWAE-MIS, shown in red) significantly improves over all of the single-proposal methods (shown in black). Notably, the performance of WW when used to learn a proposal is not as good as expected. Therefore, we ran the same experiment with a higher number of particles and reported the results in Appendix E. Briefly, WW learns the best model for 200 particles and our three-step procedure (WW-MIS) still outperforms all existing methods.

With respect to the χ -VAE, we noticed that using a Student’s t-distribution as the variational distribution (in place of the standard Gaussian distribution) usually improves the MAE. Because the Student’s t-distribution is also better theoretically motivated (the heavier tails of the Student-t distribution also help to avoid an infinite χ^2 divergence), we systematically use it in the χ -VAE for the real-world applications.

4 Classification-based decision theory

We consider the MNIST dataset [34], which includes features x for each of the images of handwritten digits and a label c . We aim to predict whether x has its label included in a given subset of digits (from zero to eight). We also allow no decision to be made for ambiguous cases (the “reject” option) [24].

We split the MNIST dataset [34] evenly between training and test datasets. For the labels 0 to 8, we use a total of 1,500 labeled examples. All images associated with label 9 are unlabelled. We assume in this experiment that the MNIST dataset has $C = 9$ classes (i.e., $c \in \{0, \dots, C-1\}$) and that we have a posterior probability for the class $p_\theta(c \mid x)$ for a model yet to be defined. Let $L(a, c)$ be the loss defined over the action set $\mathcal{A} = \{\emptyset, 0, \dots, C-1\}$. Action \emptyset is known as the rejection option in classification (we wish to reject label 9 at decision time). For this loss, it is known that the optimal decision $a^*(x)$ is a threshold-based rule [24] on the posterior probability. This setting is fundamentally different than traditional classification because making an informed decision requires knowledge of the full posterior $p_\theta(c \mid x)$ and not only the maximum probability class. This rule is a posterior expectation $\mathcal{Q}(f, x)$ for $z = c$ and f a constant unit function. We provide a complete

Table 2: Results for the M1+M2 model on MNIST. AUPRC refers to the area under of the PR curve for rejecting the label 9.

	VAE	IWAE	WW	χ -VAE
IWELBO	-104.74	-101.92	-102.82	-105.29
PSIS	$\gtrsim 1$	$\gtrsim 1$	$\gtrsim 1$	$\gtrsim 1$
AUPRC	0.35	0.45	0.29	0.44

description of the experimental setup, as well as derivations for the plugin and the SNIS estimator in Appendix F. To our knowledge, this is the first time semi-supervised generative models have been evaluated in a rejection-based decision-making scenario.

As a generative model, we use the M1+M2 model for semi-supervised learning [35]. In the M1+M2 model, the discrete latent variable c represents the class. Latent variable u is a low-dimensional vector encoding additional variation (not contained in c). Latent variable z is a low-dimensional representation of the observation, drawn from a mixture distribution with mixture assignment c and mixture parameters that are a function of u . The generative model is

$$p_\theta(x, z, c, u) = p_\theta(x | z)p_\theta(z | c, u)p_\theta(c)p_\theta(u). \quad (10)$$

The variational distribution factorizes as

$$q_\phi(z, c, u | x) = q_\phi(z | x)q_\phi(c | z)q_\phi(u | z, c). \quad (11)$$

Because the reverse KL divergence can cover only one mode of the distribution, it is more prone to attributing zero probabilities to many classes while alternate divergences would penalize this behavior. Appendix G provides further detail as to why the M1+M2 model trained as a VAE be overconfident and why WW and the χ -VAE have the potential to remedy these problems. To simplify the derivation of updates for the M1+M2 model with all of the algorithms we consider, we use the Gumbel-softmax trick [36] for latent variable c for unlabelled observations. We fit an M1+M2 model with only nine classes and consider as ground truth that images with label 9 should be rejected at decision time.

Table 2 gives our results, including the Area Under the Precision-Recall Curve (AUPRC) for classifying “nines”, as well as goodness-of-fit metrics. IWAE and WW learn the best generative model in terms of IWELBO. For all methods, we compare the classification performance of the plugin and the SNIS estimator on labels 1 through 8. While the plugin estimator shows high accuracy across all methods (between 95% and 97%), the SNIS estimator shows poor performance (around 60%). This may be because the PSIS diagnosis estimates are greater than one for all algorithms, which indicates that the variational distribution may lead to large estimation error if used as a proposal [25]. Consequently, we report the result of the plugin estimator for all algorithms in this experiment. Figure 3 shows the results of applying different variational distribution for a fixed model. These results suggest that using the χ -VAE or MIS on a fixed model leads to better decisions. In particular, our three-step procedure (IWAE-MIS) outperforms all single-proposal alternatives.

5 Multiple testing and differential gene expression

We present an experiment involving Bayesian hypothesis testing for detecting differentially expressed genes from single-cell transcriptomics data, a central problem in modern molecular biology. Single-cell RNA sequencing data (scRNA-seq) provides a noisy snapshot of the gene expression levels of cells [37, 38]. It can reveal cell types and gene markers for each cell type as long as we have an accurate noise model [39]. scRNA-seq data is a cell-by-gene matrix X . For cell $n = 1, \dots, N$ and gene $g = 1, \dots, G$, entry X_{ng} is the number of transcripts for gene g observed in cell n . Here we take as given that each cell comes paired with an observed cell-type label c_n .

Single-cell Variational Inference (scVI) [7] is a hierarchical Bayes model [26] for scRNA-seq data. For our purposes here, it suffices to know that the latent variables h_{ng} represent the underlying gene expression level for gene g in cell n , corrected for a certain number of technical variations (e.g., sequencing depth effects). The corrected expression levels h_{ng} are more reflective of the real

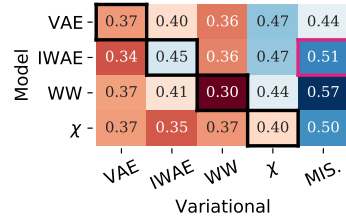


Figure 3: AUPRC on MNIST for combinations of VAEs (row) and inference only (columns) frameworks.

Table 3: Results for the scVI model. MAE FDR refers to the mean absolute error for FDR estimation.

	VAE	IWAE	WW	χ-VAE
AIS	-380.42	-372.86	-372.78	-371.69
IWELBO	-380.42	-372.86	-372.78	-371.69
PSIS	0.71	0.49	0.47	0.69
MAE FDR	5.78	0.39	0.51	0.27

proportion of gene expression than the raw data X [40]. Log-fold changes based on h_{ng} can be used to detect differential expression (DE) of gene g across cell types a and b [41, 42]. Indeed, Bayesian decision theory helps decide between a model of the world \mathcal{M}_1^g in which gene g is DE and an alternative model \mathcal{M}_0^g of non-DE. The hypotheses are

$$\mathcal{M}_1^g : \left| \log \frac{h_{ag}}{h_{bg}} \right| \geq \delta \quad \text{and} \quad \mathcal{M}_0^g : \left| \log \frac{h_{ag}}{h_{bg}} \right| < \delta, \quad (12)$$

where δ is a threshold defined by the practitioner. DE can therefore be performed by posterior estimation of log-fold change between two cells x_a, x_b , which can be written as $p_\theta(\mathcal{M}_1^g | x_a, x_b)$ and estimated with importance sampling. The optimal decision rule for 0-1 loss is attained by thresholding the posterior log-fold change estimate. Rather than directly setting this threshold, a practitioner typically picks a false discovery rate (FDR) f_0 to target. For controlling the FDR, we consider the multiple binary decision rule $\mu^k = (\mu_g^k, g \in G)$ that consists of tagging DE the k genes with the highest posterior estimate of log-fold change. With this notation, the false discovery proportion (FDP) of such a decision rule is

$$\text{FDP} = \frac{\sum_g (1 - \mathcal{M}_1^g) \mu_g^k}{\sum_g \mu_g^k}. \quad (13)$$

Following [43], we define the posterior expected FDR as $\overline{\text{FDR}} := \mathbb{E} [\text{FDP} | x_a, x_b]$, which can be computed from the differential expression probabilities of Eq. (12). We then set k so that it is the maximum value for which the posterior expected FDR is below f_0 . In this case, controlling the FDR requires estimating G posterior expectations. To quantify the success of a given method at controlling the FDR at any arbitrary level, we will report the mean absolute error between the groundtruth FDR and the posterior expected FDR.

We fit the scVI model with all the objective functions of interest. In addition, we also use annealed importance sampling (AIS) [27] to approximate the posterior distribution once the model is fitted. AIS is computationally intensive, so we used 500 steps and 100 samples from the prior to keep a reasonable runtime. Because the ground-truth FDR cannot be computed on real data, we generated scRNA-seq data according to a Poisson Log-Normal model (a popular choice for simulating scRNA-seq data [44, 45]) from five distinct cells types corresponding to 10,000 cells and 100 genes. This model is meant to reflect both biological signal and technicalities of the experimental protocol. We provide further details about this experiment in Appendix H.

VAE performs worse in terms of held-out log-likelihood (both IWELBO and AIS), while χ -VAE performs best (Table 3). We also evaluate the quality of the gene ranking for differential expression, based on the AUPRC of the DE probabilities. The model learned with the VAE objective function has an AUPRC of 0.85 while all other combinations have an AUPRC of more than 0.95.

Next, we investigate the role posterior uncertainty plays in properly estimating the FDR. Table 3 and Figure 4 report the mean absolute error (MAE) for FDR estimation over the 100 genes. The posterior expected FDR has a large error for any proposal based on the VAE model, that gets even worse using the plugin estimator. However, all the other models yield a significantly lower error (from 1 to 2%), for any proposal. We provided the FDR curves in Appendix H. The VAE has highly inaccurate FDR control while IWAE, WW and χ -VAE may be useful to a practitioner, also with some error. This suggests that the model learned by the original scVI training procedure (i.e., a VAE) cannot be used for FDR control, even using AIS to find a proposal. Furthermore, in this experiment WW slightly outperforms IWAE in terms of held-out IWELBO but not in terms of MAE FDR. Again, the variational distribution used to train the best generative model does not necessarily provide the best

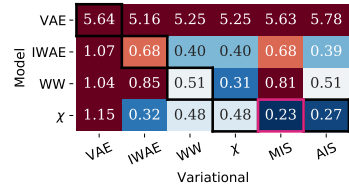


Figure 4: MAE FDR for scVI: combinations of VAEs (row) and inference only (columns) frameworks.

decisions. Conversely, our three-step procedure (χ -VAE-MIS) has the best FDR estimates on this experiment, improving over all the single-proposal alternatives as well as χ -VAE followed by AIS.

6 Discussion

We have proposed a three-step procedure for using variational autoencoders for decision-making. This is theoretically motivated by analyzing the derived error of the SNIS estimator and the biases of variational Bayes on the pPCA model. Our numerical experiments show that in important real-world examples this three-step procedure outperforms the VAE, IWAE, WW, the χ -VAE, but also IWAE followed by AIS.

The proposed procedure requires to fit three VAEs, each with a different loss function. This causes a computational overhead of our method compared to a standard VAE. However, this overhead is not large (roughly a constant factor of three) since our method simply consists of training three VAEs, each with a different loss function. In the pPCA experiment, training a single VAE takes 12 seconds while fitting step 1 and 2 of our method takes 53 seconds (on a machine with a single NVIDIA GeForce RTX 2070 GPU). Step 3 does not introduce any additional computations. In cases where an offline decision is made (for example in biology), we do not expect the overhead of our method to be a bottleneck.

A related issue to fitting VAEs, an important step of our work, is the posterior collapse phenomenon. For example, when the decoder network is too flexible, the model might ignore the latent variables. While a complete treatment of posterior collapse is largely beyond the scope of this work, we proposed follow-up experiments in the pPCA example in Appendix E. Briefly, we added to the benchmark two methods proposed to mitigate this problem, cyclical annealing [46] and lagging inference networks [47]. While we do note substantial improvement of the VAE baseline, these two methods are largely outperformed by the approaches we proposed in this manuscript.

A complementary approach to decision-making is the elegant framework of loss-calibrated inference [48, 49], which further adapts the ELBO to take into account the loss function L . Similarly, amortized Monte Carlo integration [50] proposes to fit a variational distribution with a model and a target in mind. We note that both frameworks are not directly applicable because adapting the ELBO for a specific decision-making loss implies a significant bias in learning p_θ . However, these could potentially improve step 2 and 3 of our proposed framework. Indeed, both approaches rely on the reverse KL divergence but alternative divergences could be explored, as we did in this manuscript. Consequently, developing hybrid algorithms is a promising direction for future research.

Broader Impact

The method we propose lets people make better decisions based on data. This capability may improve decisions about topics as diverse as differential expression in biological data, supply chain inventory and pricing, and personalized medicine treatments. The black-box nature of neural networks, however, which is a key aspect of our approach, confers both benefits and risks. For data without a simple parametric distribution, neural networks let us fit a model it accurately, so that we can make decisions in a rigorous data-driven way without recreating prior biases. However, it can be difficult to check the quality of the model fit, particularly when worst-case analysis is appropriate; e.g. in mission-critical applications. In VAE-style architectures, powerful decoder networks are associated with posterior collapse, which could go undetected. More research is needed to ensure the worst-case performance of VAE-style models and/or to diagnosis fit problems before high-stakes decisions are based on them. More work is also needed to ensure the models we fit identify causal links, not associations.

Acknowledgments and Disclosure of Funding

We thank Chenling Xu for suggestions that helped with the third experiment. We thank Adam Kosiorek and Tuan-Anh Le for answering questions about implementation of the Wake-Wake algorithm. We thank Geoffrey Negiar, Adam Gayoso and Achille Nazaret for their feedback about this article. NY and RL were supported by grant U19 AI090023 from NIH-NIAID.

References

- [1] Diederik P Kingma and Max Welling. Auto-encoding variational Bayes. In *International Conference on Learning Representations*, 2014.
- [2] Danilo Jimenez Rezende, Shakir Mohamed, and Daan Wierstra. Stochastic backpropagation and approximate inference in deep generative models. In *International Conference on Machine Learning*, 2014.
- [3] Ishaan Gulrajani, Kundan Kumar, Faruk Ahmed, Adrien Ali Taiga, Francesco Visin, David Vazquez, and Aaron Courville. PixelVAE: a latent variable model for natural images. In *International Conference on Learning Representations*, 2017.
- [4] Alexander Amini, Brandon Araki, Daniela Rus, Wilko Schwarting, Guy Rosman, Sertac Karaman, and Daniela L Rus. Variational autoencoder for end-to-end control of autonomous driving with novelty detection and training de-biasing. In *International Conference on Intelligent Robots and Systems*, 2018.
- [5] Adam J. Riesselman, John B. Ingraham, and Debora S. Marks. Deep generative models of genetic variation capture the effects of mutations. *Nature Methods*, 2018.
- [6] Jiarui Ding, Anne Condon, and Sohrab P Shah. Interpretable dimensionality reduction of single cell transcriptome data with deep generative models. *Nature communications*, 2018.
- [7] Romain Lopez, Jeffrey Regier, Michael B. Cole, Michael I. Jordan, and Nir Yosef. Deep generative modeling for single-cell transcriptomics. *Nature Methods*, 2018.
- [8] Chenling Xu, Romain Lopez, Edouard Mehlman, Jeffrey Regier, Michael I. Jordan, and Nir Yosef. Probabilistic harmonization and annotation of single-cell transcriptomics data with deep generative models. *bioRxiv*, 2019.
- [9] James Berger. *Statistical Decision Theory and Bayesian Analysis*. Springer Science, 1985.
- [10] Justin Domke and Daniel R Sheldon. Importance weighting and variational inference. In *Advances in Neural Information Processing Systems*, 2018.
- [11] Yuhuai Wu, Yuri Burda, Ruslan Salakhutdinov, and Roger Grosse. On the quantitative analysis of decoder-based generative models. In *International Conference on Learning Representations*, 2017.
- [12] Martin J Wainwright and Michael I Jordan. Graphical models, exponential families, and variational inference. *Foundations and Trends in Machine Learning*, 2008.
- [13] Richard Eric Turner and Maneesh Sahani. Two problems with variational expectation maximisation for time-series models. Technical report, Gatsby Computational Neuroscience Unit, 2011.
- [14] Thomas P Minka. Expectation propagation for approximate bayesian inference. In *Uncertainty in Artificial Intelligence*, 2001.
- [15] Adji Bousso Dieng, Dustin Tran, Rajesh Ranganath, John Paisley, and David Blei. Variational inference via chi-square upper bound minimization. In *Advances in Neural Information Processing Systems*, 2017.
- [16] Sourav Chatterjee and Persi Diaconis. The sample size required in importance sampling. *The Annals of Applied Probability*, 2018.
- [17] Sergios Agapiou, Omiros Papaspiliopoulos, Daniel Sanz-Alonso, and Andrew Stuart. Importance sampling: Intrinsic dimension and computational cost. *Statistical Science*, 2017.
- [18] Yuri Burda, Roger B. Grosse, and Ruslan Salakhutdinov. Importance weighted autoencoders. In *International Conference on Learning Representations*, 2016.
- [19] Tom Rainforth, Adam Kosiorek, Tuan Anh Le, Chris Maddison, Maximilian Igl, Frank Wood, and Yee Whye Teh. Tighter variational bounds are not necessarily better. In *International Conference on Machine Learning*, 2018.
- [20] Liqun Chen, Chenyang Tao, Ruiyi Zhang, Ricardo Henao, and Lawrence Carin Duke. Variational inference and model selection with generalized evidence bounds. In *International Conference on Machine Learning*, 2018.
- [21] Jörg Bornschein and Yoshua Bengio. Reweighted wake-sleep. In *International Conference on Learning Representations*, 2015.
- [22] Tuan Anh Le, A Kosiorek, N Siddharth, Yee Whye Teh, and Frank Wood. Revisiting reweighted wake-sleep for models with stochastic control flow. *Uncertainty in Artificial Intelligence*, 2019.
- [23] Eric Veach and Leonidas J Guibas. Optimally combining sampling techniques for Monte Carlo rendering. In *Proceedings of the 22nd annual conference on Computer graphics and interactive techniques*, 1995.
- [24] Christopher M. Bishop. *Pattern Recognition and Machine Learning*. Springer-Verlag, 2006.
- [25] Yuling Yao, Aki Vehtari, Daniel Simpson, and Andrew Gelman. Yes, but did it work?: Evaluating variational inference. In *International Conference on Machine Learning*, 2018.

[26] Andrew Gelman and Jennifer Hill. *Data Analysis Using Regression and Multilevel/Hierarchical Models*. Cambridge University Press, 2007.

[27] Radford M Neal. Annealed importance sampling. *Statistics and computing*, 2001.

[28] Corinna Cortes, Yishay Mansour, and Mehryar Mohri. Learning bounds for importance weighting. In *Advances in Neural Information Processing Systems*, 2010.

[29] Michael E Tipping and Christopher M Bishop. Probabilistic principal component analysis. *Journal of the Royal Statistical Society: Series B (Statistical Methodology)*, 1999.

[30] Pierre Simon Laplace. Memoir on the probability of the causes of events. *Statistical Science*, 1986.

[31] Martin J. Wainwright. *High-Dimensional Statistics: A Non-Asymptotic Viewpoint*. Cambridge University Press, 2019.

[32] Art B. Owen. *Monte Carlo Theory, Methods and Examples*. 2013.

[33] Tim Hesterberg. Weighted average importance sampling and defensive mixture distributions. *Technometrics*, 1995.

[34] Yann LeCun, Léon Bottou, Yoshua Bengio, Patrick Haffner, et al. Gradient-based learning applied to document recognition. *Proceedings of the IEEE*, 1998.

[35] Diederik P Kingma, Shakir Mohamed, Danilo Jimenez Rezende, and Max Welling. Semi-supervised learning with deep generative models. In *Advances in Neural Information Processing Systems*, 2014.

[36] Eric Jang, Shixiang Gu, and Ben Poole. Categorical reparametrization with Gumble-Softmax. In *International Conference on Learning Representations*, 2017.

[37] Allon Wagner, Aviv Regev, and Nir Yosef. Revealing the vectors of cellular identity with single-cell genomics. *Nature Biotechnology*, 2016.

[38] Amos Tanay and Aviv Regev. Scaling single-cell genomics from phenomenology to mechanism. *Nature*, 2017.

[39] Dominic Grun, Lennart Kester, and Alexander van Oudenaarden. Validation of noise models for single-cell transcriptomics. *Nature Methods*, 2014.

[40] Michael B Cole, Davide Rissi, Allon Wagner, David DeTomaso, John Ngai, Elizabeth Purdom, Sandrine Dudoit, and Nir Yosef. Performance assessment and selection of normalization procedures for single-cell RNA-seq. *Cell Systems*, 2017.

[41] Michael I. Love, Wolfgang Huber, and Simon Anders. Moderated estimation of fold change and dispersion for RNA-seq data with DESeq2. *Genome Biology*, 2014.

[42] Pierre Boyneau, Romain Lopez, Jeffrey Regier, Adam Gayoso, Michael I. Jordan, and Nir Yosef. Deep generative models for detecting differential expression in single cells. In *Machine Learning in Computational Biology*, 2019.

[43] Shiqi Cui, Subharup Guha, Marco A. R. Ferreira, and Allison N. Tegge. hmmSeq: A hidden Markov model for detecting differentially expressed genes from RNA-seq data. *The Annals of Applied Statistics*, 2015.

[44] F William Townes, Stephanie C Hicks, Martin J Aryee, and Rafael A Irizarry. Feature selection and dimension reduction for single-cell RNA-Seq based on a multinomial model. *Genome biology*, 2019.

[45] Helena L. Crowell, Charlotte Soneson, Pierre-Luc Germain, Daniela Calini, Ludovic Collin, Catarina Raposo, Dheeraj Malhotra, and Mark D. Robinson. On the discovery of subpopulation-specific state transitions from multi-sample multi-condition single-cell RNA sequencing data. *bioRxiv*, 2020.

[46] Hao Fu, Chunyuan Li, Xiaodong Liu, Jianfeng Gao, Asli Celikyilmaz, and Lawrence Carin. Cyclical annealing schedule: a simple approach to mitigating KL vanishing. In *Conference of the North American Chapter of the Association for Computational Linguistics: Human Language Technologies*, 2019.

[47] Junxian He, Daniel Spokoyn, Graham Neubig, and Taylor Berg-Kirkpatrick. Lagging inference networks and posterior collapse in variational autoencoders. In *International Conference on Learning Representations*, 2018.

[48] Simon Lacoste-Julien, Ferenc Huszár, and Zoubin Ghahramani. Approximate inference for the loss-calibrated Bayesian. In *International Conference on Artificial Intelligence and Statistics*, 2011.

[49] Tomasz Kuśmierczyk, Joseph Sakaya, and Arto Klami. Variational Bayesian decision-making for continuous utilities. In *Advances in Neural Information Processing Systems*, 2019.

[50] Adam Golinski, Frank Wood, and Tom Rainforth. Amortized Monte Carlo integration. In *International Conference on Machine Learning*, 2019.

[51] Beatrice Laurent and Pascal Massart. Adaptive estimation of a quadratic functional by model selection. *The Annals of Statistics*, 2000.

- [52] Futoshi Futami, Issei Sato, and Masashi Sugiyama. Variational inference based on robust divergences. In *International Conference on Artificial Intelligence and Statistics*, 2018.
- [53] Mikhail Figurnov, Shakir Mohamed, and Andriy Mnih. Implicit reparameterization gradients. In *Advances in Neural Information Processing Systems*, 2018.
- [54] Yingzhen Li and Richard E Turner. Rényi divergence variational inference. In *Advances in Neural Information Processing Systems*, 2016.
- [55] Jacob Burbea. The convexity with respect to Gaussian distributions of divergences of order α . *Utilitas Mathematica*, 1984.
- [56] Yunchen Pu, Zhe Gan, Ricardo Henao, Xin Yuan, Chunyuan Li, Andrew Stevens, and Lawrence Carin. Variational autoencoder for deep learning of images, labels and captions. In *Advances in Neural Information Processing Systems*, 2016.
- [57] James Lucas, George Tucker, Roger B Grosse, and Mohammad Norouzi. Don't blame the ELBO! a linear VAE perspective on posterior collapse. In *Advances in Neural Information Processing Systems*, 2019.
- [58] Günter Klambauer, Thomas Unterthiner, Andreas Mayr, and Sepp Hochreiter. Self-normalizing neural networks. In *Advances in Neural Information Processing Systems*, 2017.
- [59] Chuan Guo, Geoff Pleiss, Yu Sun, and Kilian Q. Weinberger. On calibration of modern neural networks. In *International Conference on Machine Learning*, 2017.

Supplementary Information

In Appendix A, we prove the theoretical results presented in this manuscript. In Appendix B, we present details for the χ -VAE. In Appendix C we provide known bounds for posterior expectation estimators. In Appendix D, we present the analytical derivations in the bivariate Gaussian setting. In Appendix E and F, we provide the experimental details for the pPCA and the MNIST experiment. In Appendix G, we discuss why alternative divergences would be especially suitable for the M1+M2 model. In Appendix H, we present additional information about the single-cell transcriptomics experiment.

A Proofs

A.1 Proof of Lemma 1

Lemma 1. (Concentration of the log-likelihood ratio) *For an observation x , let Σ be the variance of the posterior distribution under the pPCA model, $p_\theta(z | x)$. Let*

$$A(x) = \Sigma^{1/2} [D(x)]^{-1} \Sigma^{1/2} - I. \quad (6)$$

For z following the posterior distribution, $\log w(x, z)$ is a sub-exponential random variable. Further, there exists a $t^(x)$ such that, under the posterior $p_\theta(z | x)$ and for all $t > t^*(x)$,*

$$\mathbb{P}(|\log w(x, z) - \Delta_{KL}(p_\theta \| q_\phi)| \geq t) \leq e^{-\frac{t}{8\|A(x)\|_2}}. \quad (7)$$

Proof. Here we first give the closed-form expression of the posterior and then we prove the concentration bounds on the log-likelihood ratio. Let $M = W^\top W + \sigma^2 I$. For notational convenience, we do not explicitly denote dependence on random variable x .

Step 1: Tractable posterior. Using the Gaussian conditioning formula [24], we have that

$$p_\theta(z | x) = \text{Normal}(M^{-1}W^\top(x - \mu), \sigma^2 M^{-1}). \quad (14)$$

Step 2: Concentration of the log-ratio. For this, since x is a fixed point, we note $a = M^{-1}W^\top(x - \mu)$ and $b = \nu(x)$. We can express the log density ratio as

$$w(z, x) = \log \frac{p_\theta(z | x)}{q_\phi(z | x)} \quad (15)$$

$$= -\frac{1}{2} \log \det(\sigma^2 M^{-1} D^{-1}) - \frac{1}{2\sigma^2} (z - a)^\top M(z - a) + \frac{1}{2} (z - b)^\top D^{-1} (z - b) \quad (16)$$

$$= C + z^\top \left[\frac{D^{-1}}{2} - \frac{M}{2\sigma^2} \right] z + \left[D^{-1} b - \frac{M a}{\sigma^2} \right]^\top z, \quad (17)$$

where C is a constant. To further characterize the tail behavior, let ϵ be an isotropic multivariate normal distribution and express the log-ratio as a function of ϵ instead of the posterior probability. We have that $z = M^{-1}W^\top(x - \mu) + \sigma M^{-1/2} \epsilon$. The log ratio can now be written as

$$\log w(z, x) = C' + \epsilon^\top \left[\frac{\sigma^2 M^{-1/2} D^{-1} M^{-1/2} - I}{2} \right] \epsilon + \left[\sigma M^{-1/2} D^{-1} b - \frac{M^{1/2} a}{\sigma} \right]^\top \epsilon. \quad (18)$$

Because ϵ is isotropic Gaussian, we can compute the deviation of this log-ratio and provide concentration bounds. Because ϵ is Gaussian and $\epsilon \mapsto \log w(z, x)$ is a quadratic function, we show the log-ratio under the posterior is a sub-exponential random variable.

The following Lemma makes this statement precise, and it has a similar implication as the classic result in [51].

Lemma 2. *Let $d \in \mathbb{N}^*$ and $\epsilon \sim \text{Normal}(0, I_d)$. For matrix $A \in \mathbb{R}^{d \times d}$ and vector $b \in \mathbb{R}^d$, random variable $v = \epsilon^\top A \epsilon + b^\top \epsilon$ is sub-exponential with parameters $(\sqrt{2 \|A\|_F^2 + \|b\|_2^2 / 4}, 4 \|A\|_2)$. In particular, we have the following concentration bounds,*

$$\mathbb{P}[|v| \geq t] \leq 2 \exp \left\{ -\frac{t^2}{8 \|A\|_F^2 + \|b\|_2^2 + 4 \|A\|_2 t} \right\} \quad \text{for all } t > 0. \quad (19)$$

$$\mathbb{P}[|v| \geq t] \leq \exp \left\{ -\frac{t}{8 \|A\|_2} \right\} \quad \text{for all } t > \frac{8 \|A\|_F^2 + \|b\|_2^2}{16 \|A\|_2}. \quad (20)$$

For $A = \frac{\sigma^2 M^{-1/2} D^{-1} M^{-1/2} - I}{2}$ and $b = \sigma M^{-1/2} D^{-1} b - \frac{M^{1/2} a}{\sigma}$, we can apply Lemma 2. We deduce a concentration bound on the log-ratio around its mean, which is the forward Kullback-Leibler divergence $L = \Delta_{\text{KL}}(p_\theta(z|x) \| q_\phi(z|x))$. More precisely, we have that

$$p_\theta(|\log w(z, x) - L| \geq t | x) \leq 2 \exp \left\{ -\frac{t^2}{8 \|A\|_F^2 + \|b\|_2^2 + 4 \|A\|_2 t} \right\} \quad \text{for all } t > 0. \quad (21)$$

□

as well as the deviation bound for large t , which ends the proof.

A.2 Proof of Lemma 2

Proof. Let $\lambda \in \mathbb{R}^+$. We have that $\mathbb{E}v = \text{Tr}(A)$. We wish to bound the moment generating function

$$\mathbb{E}[e^{\lambda(v - \text{Tr}(A))}] = e^{-\lambda \text{Tr}(A)} \mathbb{E}[e^{\lambda(\epsilon^\top A \epsilon + b^\top \epsilon)}]. \quad (22)$$

Sums of arbitrary correlated variables are hard to analyze. Here we rely on the property that Gaussian vectors are invariant by rotation: Let $A = Q\Lambda Q^\top$ be the eigenvalue decomposition for A and denote $\epsilon = Q\xi$ as well as $b = Q\beta$. Since Q is an orthogonal matrix, ξ also follows an isotropic normal distribution and

$$\mathbb{E}[e^{\lambda(v - \text{Tr}(A))}] = e^{-\lambda \text{Tr}(A)} \mathbb{E}[e^{\lambda(\xi^\top \Lambda \xi + \beta^\top \xi)}] \quad (23)$$

$$= e^{-\lambda \text{Tr}(A)} \mathbb{E}\left[\prod_{i=1}^d e^{\lambda \xi_i^2 \Lambda_i + \lambda \beta_i \xi_i}\right] \quad (24)$$

$$= e^{-\lambda \text{Tr}(A)} \prod_{i=1}^d \mathbb{E}\left[e^{\lambda \xi_i^2 \Lambda_i + \lambda \beta_i \xi_i}\right] \quad (25)$$

$$= \prod_{i=1}^d \mathbb{E}\left[e^{\lambda \xi_i^2 \Lambda_i + \lambda \beta_i \xi_i - \lambda \Lambda_i}\right]. \quad (26)$$

Because each component ξ_i follows a isotropic Gaussian distribution, we can compute the moment generating functions in closed form

$$\mathbb{E}\left[e^{\lambda \xi_i^2 \Lambda_i + \lambda \beta_i \xi_i - \lambda \Lambda_i}\right] = \frac{e^{-\lambda \Lambda_i}}{\sqrt{2\pi}} \int_{-\infty}^{+\infty} e^{\lambda \Lambda_i u^2 + \lambda \beta_i u} e^{-\frac{u^2}{2}} du \quad (27)$$

$$= \frac{e^{-\lambda \Lambda_i}}{\sqrt{2\pi}} \int_{-\infty}^{+\infty} e^{[\lambda \Lambda_i - \frac{1}{2}]u^2 + \lambda \beta_i u} du. \quad (28)$$

This integral is convergent if and only if $\lambda < 1/2\Lambda_i$. In that case, we have after a change of variable that

$$\mathbb{E}\left[e^{\lambda \xi_i^2 \Lambda_i + \lambda \beta_i \xi_i - \lambda \Lambda_i}\right] = \frac{e^{-\lambda \Lambda_i}}{\sqrt{\pi} \sqrt{1 - 2\lambda \Lambda_i}} \int_{-\infty}^{+\infty} e^{-s^2 + \frac{\sqrt{2}\lambda \beta_i s}{\sqrt{1 - 2\lambda \Lambda_i}}} ds \quad (29)$$

$$= \frac{e^{-\lambda \Lambda_i} e^{\frac{\lambda^2 \beta_i^2}{2(1 - 2\lambda \Lambda_i)}}}{\sqrt{1 - 2\lambda \Lambda_i}}. \quad (30)$$

Then, using the fact that for $a < 1/2$, we have $e^{-a} \leq e^{2a^2} \sqrt{1 - 2a}$, we can further simplify for $\lambda < \frac{1}{4\Lambda_i}$

$$\mathbb{E}\left[e^{\lambda \xi_i^2 \Lambda_i + \lambda \beta_i \xi_i - \lambda \Lambda_i}\right] \leq e^{2\lambda^2 \Lambda_i^2 + \frac{\lambda^2 \beta_i^2}{2(1 - 2\lambda \Lambda_i)}} \quad (31)$$

$$\leq e^{[2\Lambda_i^2 + \frac{\beta_i^2}{4}]\lambda^2}. \quad (32)$$

Putting back all the components of ξ , we have that for all $\lambda < \frac{1}{4\|\Lambda\|_2} = \frac{1}{4\|A\|_2}$

$$\mathbb{E}[e^{\lambda(v - \text{Tr}(A))}] \leq \exp \left\{ \left[2\|\Lambda\|_F^2 + \frac{\|\beta\|_2^2}{4} \right] \lambda^2 \right\} \quad (33)$$

$$\leq \exp \left\{ \left[2\|A\|_F^2 + \frac{\|b\|_2^2}{4} \right] \lambda^2 \right\}, \quad (34)$$

where the last inequality is in fact an equality because Q is an isometry. Therefore, according to Definition 2.2 in [31], v is sub-exponential with parameters $(\sqrt{2\|A\|_F^2 + \|b\|_2^2/4}, 4\|A\|_2)$. The concentration bound is derived as in the proof of Proposition 2.3 in [31]. \square

A.3 Proof of Theorem 1

Theorem 1. (Sufficient sample size) *For an observation x , suppose that the second moment of $f(z)$ under the posterior is bounded by κ . If the number of importance sampling particles n satisfies $n = \beta \exp\{\Delta_{KL}(p_\theta \| q_\phi)\}$ for some $\beta > \log t^*(x)$, then*

$$\mathbb{P}\left(\left|\hat{\mathcal{Q}}_{IS}^n(f, x) - \mathcal{Q}(f, x)\right| \geq \frac{2\sqrt{3\kappa}}{\beta^{1/s\gamma} - \sqrt{3}}\right) \leq \frac{\sqrt{3}}{\beta^{1/s\gamma}}, \quad (8)$$

with $\gamma = \max(1, 4\|A(x)\|_2)$

Proof. Let $t = \ln \beta$. By Theorem 1.2 from [16], and by Lemma 1 for $t > t^*(x)$, and

$$\epsilon = \left(e^{-\frac{t}{4}} + 2e^{-\frac{t}{16\|A(x)\|_2}}\right)^{1/2}, \quad (35)$$

we have that

$$\mathbb{P}\left(\left|\hat{\mathcal{Q}}_{IS}^n(f, x) - \mathcal{Q}(f, x)\right| \geq \frac{2\|f\|_2 \epsilon}{1 - \epsilon}\right) \leq \epsilon. \quad (36)$$

Now, let us notice that $\epsilon \leq \sqrt{3}e^{-\frac{t}{8\gamma}}$ and that $x \mapsto x/1-x$ is increasing on $(0, 1)$. So we have that

$$\mathbb{P}\left(\left|\hat{\mathcal{Q}}_{IS}^n(f, x) - \mathcal{Q}(f, x)\right| \geq \frac{2\sqrt{3\kappa}}{e^{\frac{t}{8\gamma}} - \sqrt{3}}\right) \leq \sqrt{3}e^{-\frac{t}{8\gamma}}. \quad (37)$$

The bound in Theorem 1 follows by replacing e^t by β in the previous equation. \square

B Chi-VAEs

We propose a novel variant of the WW algorithm based on χ^2 divergence minimization, and thus potentially particularly suited for decision-making. This variant is incremental in the sense that it combines several existing contributions such as the CHIVI procedure [15], the WW algorithm [22] as well as using a reparameterized Student’s t distributed variational posterior (e.g., explored in [10] for IWVI). However, we did not encounter any other mention of such a variant in previous literature.

In the χ -VAE, we update the model and the variational parameters as a first-order stochastic block coordinate descent (as in WW [22]). For a fixed inference model q_ϕ , we take gradients of the IWELBO with respect to the model parameters. For a fixed generative model p_θ , we seek to minimize the χ^2 divergence between the posterior and the inference model. This quantity is intractable but we can formulate an equivalent optimization problem using the χ upper bound (CUBO) [15]:

$$\underbrace{\log p_\theta(x)}_{\text{evidence}} = \underbrace{\frac{1}{2} \log \mathbb{E}_{q_\phi(z|x)} \left(\frac{p_\theta(x, z)}{q_\phi(z|x)} \right)^2}_{\text{CUBO}} - \underbrace{\frac{1}{2} \log (1 + \Delta_{\chi^2}(p_\theta \| q_\phi))}_{\chi^2 \text{ VG}}. \quad (38)$$

It is known that the properties of the variational distribution (mode-seeking or mass-covering) depends highly on the geometry of the variational gap [52], which was our initial motivation for using the χ -VAE for decision-making. For a fixed model, minimizing the exponentiated CUBO is a valid approach for minimizing the χ^2 divergence.

Finally, in many cases the χ^2 divergence may be infinite. This is true even for two Gaussian distributions provided that the variance of q_ϕ does not cover the posterior enough. We found in our pPCA experiments that using a Gaussian distributed posterior may still provide helpful proposals. However, we expect a Student’s t distributed variational posterior to properly alleviate this concern. [10] proposed a reparameterization trick for elliptical distributions, including the Student’s t

distribution based on the CDF of the χ distribution. In our experiments, we reparameterized samples from a Student's t distribution with location μ , scale $\Sigma = A^\top A$ and degrees of freedom ν as follows:

$$\delta \sim \text{Normal}(0, I) \quad (39)$$

$$\epsilon \sim \chi_\nu^2 \quad (40)$$

$$t \sim \sqrt{\frac{\nu}{\epsilon}} A^\top \delta + \mu, \quad (41)$$

where we used reparameterized samples for the χ_ν^2 distribution following [53].

C Limitations of standard results for posterior statistics estimators

Neither [16] nor [17] pretended that upper bounds on the error of the IS estimator may help comparing algorithmic procedures. Similarly, [22] used the result from [16] as a motivation but did not use it to claim better performance than another method. Still, we outline two simple reasons in this section for why upper bounds on the error of IS are not helpful for comparing algorithms.

We start by stating simple results of upper bounding the mean square error of the SNIS estimator.

Proposition 1. (Deviation for posterior expectation estimates) *Let f be a bounded test function. For the plugin estimator, we have*

$$\sup_{\|f\|_\infty \leq 1} \mathbb{E} \left[(\hat{Q}_P^n(f, x) - Q(f, x))^2 \right] \leq 4\Delta_{TV}^2(p_\theta, q_\phi) + \frac{1}{2n}, \quad (42)$$

where Δ_{TV} denotes the total variation distance. For the SNIS estimator, if we further assume that $w(x, z)$ has finite second order moment under $q_\phi(z | x)$, then we have

$$\sup_{\|f\|_\infty \leq 1} \mathbb{E} \left[(\hat{Q}_{IS}^n(f, x) - Q(f, x))^2 \right] \leq \frac{4\Delta_{\chi^2}(p_\theta \| q_\phi)}{n}, \quad (43)$$

where Δ_{χ^2} denotes the chi-square divergence.

We derive the first bound is derived in a later section while the second one is from [17]. We now derive two points to argue that such bounds are uninformative for selecting the best algorithm.

First, these bounds suggest the plugin estimator is suboptimal because its bias does not vanish with infinite samples, in contrast to the SNIS estimator. However, the upper bound in [17] may be uninformative when the χ^2 divergence is infinite (as it may be for a VAE). Consequently, it is not immediately apparent which estimator will perform better.

A second issue we wish to underline pertains to the general fact that upper bounds may be loose. For example, with Pinsker's inequality we may further upper bound the bias of the plugin estimator by the square root of either $\Delta_{KL}(p_\theta \| q_\phi)$ or $\Delta_{KL}(q_\phi \| p_\theta)$. In which case, the VAE and the WW algorithm [22] both minimize an upper bound on the mean-square error of the plugin estimator; which one to choose is again not clear.

C.1 Proof of Proposition 1

Proposition 1. (Deviation for posterior expectation estimates) *Let f be a bounded test function. For the plugin estimator, we have*

$$\sup_{\|f\|_\infty \leq 1} \mathbb{E} \left[(\hat{Q}_P^n(f, x) - Q(f, x))^2 \right] \leq 4\Delta_{TV}^2(p_\theta, q_\phi) + \frac{1}{2n}, \quad (42)$$

where Δ_{TV} denotes the total variation distance. For the SNIS estimator, if we further assume that $w(x, z)$ has finite second order moment under $q_\phi(z | x)$, then we have

$$\sup_{\|f\|_\infty \leq 1} \mathbb{E} \left[(\hat{Q}_{IS}^n(f, x) - Q(f, x))^2 \right] \leq \frac{4\Delta_{\chi^2}(p_\theta \| q_\phi)}{n}, \quad (43)$$

where Δ_{χ^2} denotes the chi-square divergence.

Proof. For the plugin estimator

$$\hat{Q}_P^n(f, x) = \frac{1}{n} \sum_{i=1}^n f(z_i), \quad (44)$$

we can directly calculate and upper bound the mean-square error. First, we will use for notational convenience:

$$I^* = \mathbb{E}_{p(z|x)} f(z) \quad (45)$$

$$\bar{I} = \mathbb{E}_{q(z|x)} f(z) \quad (46)$$

and notice that:

$$|I^* - \bar{I}| \leq \sup_{\|g\|_\infty \leq 1} |\mathbb{E}_{q(z|x)} g(z) - \mathbb{E}_{p(z|x)} g(z)| \quad (47)$$

$$\leq 2\Delta_{\text{TV}}(p(z|x), q(z|x)), \quad (48)$$

by definition of the total variation distance. Now we can proceed to the calculations:

$$\left(\frac{1}{n} \sum_{i=1}^n f(z_i) - I^* \right)^2 = \left(\frac{1}{n} \sum_{i=1}^n f(z_i) - \bar{I} \right)^2 + (I^* - \bar{I})^2 + 2 \left(\frac{1}{n} \sum_{i=1}^n f(z_i) - \bar{I} \right) (I^* - \bar{I}), \quad (49)$$

and take expectations on both sides with respect to the variational distribution:

$$\mathbb{E} \left(\frac{1}{n} \sum_{i=1}^n f(z_i) - I^* \right)^2 = \mathbb{E} \left(\frac{1}{n} \sum_{i=1}^n f(z_i) - \bar{I} \right)^2 + (I^* - \bar{I})^2 \quad (50)$$

$$= \frac{1}{n} \mathbb{E} (f(z_1) - \bar{I})^2 + (I^* - \bar{I})^2 \quad (51)$$

$$\leq \frac{1}{2n} + 4\Delta_{\text{TV}}^2(p(z|x), q(z|x)) \quad (52)$$

For the self-normalized importance sampling estimator

$$\hat{Q}_{\text{IS}}^n(f, x) = \frac{1}{n} \sum_{i=1}^n w(x, z_i) f(z_i), \quad (53)$$

we instead rely on Theorem 2.1 of [17]. \square

D Analytical derivations in the bivariate Gaussian setting

For a fixed x , we adopt the condensed notation $p_\theta(z|x) = p$. According to the Gaussian conditioning formula, there exists μ and Λ such that

$$p \sim \text{Normal}(\mu, \Lambda^{-1}).$$

We consider variational approximations of the form

$$q \sim \text{Normal}(\nu, \text{diag}(\lambda)^{-1}).$$

We wish to characterize the solution q to the following optimization problems

$$q_{\text{RKL}} = \arg \min_q \Delta_{\text{KL}}(q \| p), \quad q_{\text{FKL}} = \arg \min_q \Delta_{\text{KL}}(p \| q), \quad q_\chi = \arg \min_q \Delta_{\chi^2}(p \| q). \quad (54)$$

We focus on the setting where the mean of the variational distribution is correct. This is true for variational Bayes or the general Renyi divergence, as underlined in [54]. We therefore further assume ν can be chosen equal to μ for simplicity.

In the bivariate setting, we have conveniently an analytically tractable inverse formula:

$$\Lambda = \begin{bmatrix} \Lambda_{11} & \Lambda_{12} \\ \Lambda_{21} & \Lambda_{22} \end{bmatrix}, \quad \Lambda^{-1} = \frac{1}{|\Lambda|} \begin{bmatrix} \Lambda_{22} & -\Lambda_{12} \\ -\Lambda_{21} & \Lambda_{11} \end{bmatrix}, \quad (55)$$

We also rely on the expression of the Kullback-Leibler divergence between two multivariate Gaussian distributions of \mathbb{R}^d

$$\Delta_{\text{KL}}(\text{Normal}(\mu, \Sigma_1) \| \text{Normal}(\mu, \Sigma_2)) = \frac{1}{2} \left[\log \frac{|\Sigma_2|}{|\Sigma_1|} - d + \text{Tr}(\Sigma_2^{-1} \Sigma_1) \right]. \quad (56)$$

D.1 Reverse KL

Using the expression of the KL and the matrix inverse formula, we have that

$$\arg \min_q \Delta_{\text{KL}}(q \parallel p) = \arg \min_{\lambda_1, \lambda_2} \log \lambda_1 \lambda_2 + \frac{\Lambda_{11}}{\lambda_1} + \frac{\Lambda_{22}}{\lambda_2}. \quad (57)$$

The solution to this optimization problem is

$$\begin{cases} \lambda_1 = \Lambda_{11} \\ \lambda_2 = \Lambda_{22} \end{cases}. \quad (58)$$

D.2 Forward KL

From similar calculations,

$$\arg \min_q \Delta_{\text{KL}}(p \parallel q) = \arg \min_{\lambda_1, \lambda_2} -\log \lambda_1 \lambda_2 + \frac{1}{|\Lambda|} [\lambda_1 \Lambda_{22} + \lambda_2 \Lambda_{11}]. \quad (59)$$

The solution to this optimization problem is

$$\begin{cases} \lambda_1 = \Lambda_{11} - \frac{\Lambda_{12} \Lambda_{21}}{\Lambda_{22}} \\ \lambda_2 = \Lambda_{22} - \frac{\Lambda_{12} \Lambda_{21}}{\Lambda_{11}} \end{cases}. \quad (60)$$

D.3 Chi-square divergence

A closed-form expression of the Renyi divergence for exponential families (and in particular multivariate Gaussian) is derived in [55]. We could in principle follow the same approach. However, [56] derived a similar results, which is exactly the wanted quantity for $\alpha = -1$ in Appendix B of their manuscript. Therefore, we simply report this result

$$\begin{cases} \lambda_1 = \Lambda_{11} \left[\frac{3}{2} - \frac{1}{2} \sqrt{1 + \frac{8\Lambda_{12}\Lambda_{21}}{\Lambda_{11}\Lambda_{22}}} \right] \\ \lambda_2 = \Lambda_{22} \left[\frac{3}{2} - \frac{1}{2} \sqrt{1 + \frac{8\Lambda_{12}\Lambda_{21}}{\Lambda_{11}\Lambda_{22}}} \right] \end{cases} \quad (61)$$

D.4 Importance weighted variational inference

For IWVI, most quantities are not available in closed-form. However, the problem is simple and low-dimensional. We use naive Monte Carlo with 10,000 samples to estimate the IWELBO. The parameters λ_1, λ_2 are the solution of numerical optimization of the IWELBO (Nelder–Mead method).

E Supplemental information for the pPCA experiment

In this appendix, we give more details about the simulation, the construction of the dataset, the model as well as the neural networks architecture. We also give additional results for an increased number of particles as well as a benchmarking of posterior collapse.

E.1 Simulation

let $p, d \in \mathbb{N}^2, B = [b_1, \dots, b_p], C = [c_1, \dots, c_p], \nu \in \mathbb{R}^+$. We choose our linear system with random matrices:

$$\begin{aligned} \forall j \leq p, b_j &\sim \text{Normal} \left(0, \frac{I_d}{p} \right) \\ \forall j \leq q, c_j &\sim \text{Normal} (1, 2), \end{aligned} \quad (62)$$

and define the conditional covariance

$$\Sigma_{x|z} = \nu \times \text{diag}([c_1^2, \dots, c_p^2]). \quad (63)$$

Having drawn these parameters, the generative model is:

$$\begin{aligned} z &\sim \text{Normal}(0, I_p) \\ x | z &\sim \text{Normal}(Bz, \Sigma_{x|z}). \end{aligned} \tag{64}$$

The marginal log-likelihood $p(x)$ is tractable:

$$x \sim \text{Normal}(0, \Sigma_{x|z} + BB^\top). \tag{65}$$

The posterior $p(z | x)$ is also tractable:

$$\begin{aligned} \Sigma_{z|x}^{-1} &= I_p + A^\top \Sigma_{x|z}^{-1} A \\ M_{z|x} &= \Sigma_{z|x} A^\top \Sigma_{x|z}^{-1} \\ z | x &\sim \text{Normal}(M_{z|x} x, \Sigma_{z|x}). \end{aligned} \tag{66}$$

The posterior expectation for a toy hypothesis testing $p(z_1 \geq \nu | x)$ (with $f : z \mapsto \mathbb{1}_{\{z_1 \geq \nu\}}$) is tractable too because this distribution is Gaussian and has a tractable cumulative distribution function.

E.2 Dataset

We sample 1000 datapoints from the generative model (Equation 64) with $p = 10$, $q = 6$, and $\nu = 1$. We split the data with a 80% train - 20% test ratio.

E.3 Model details and neural networks architecture

For every baseline, we partially learned the generative model of Eq. (64). The matrix B was fixed, but the conditional diagonal covariance $\Sigma_{x|z}$ weights set as free parameters during inference. Neural networks with one hidden layer (size 128), using ReLu activations, parameterized the encoded variational distributions.

Each model was trained for 100 epochs, and optimization performed using the Adam optimizer (learning rate of 0.01, batch size 128).

E.4 Additional results

We compare PSIS levels for the pPCA dataset for each model (figure 5). For most models (IWAE, WW, and χ), the VAE variational distribution provides poor importance-weighted estimates. The PSIS exceeds 0.7 for those combinations, hinting that associated samples may be unreliable. Most other combinations show acceptable PSIS levels, with the proposals from χ and MIS performing best.

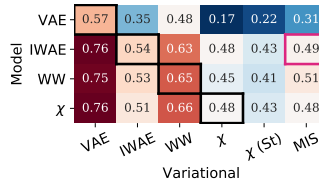


Figure 5: PSIS for pPCA: combinations of VAEs (row) and inference only (columns) frameworks.

E.5 Results with an increased number of particles

We also benchmark the different algorithms for an increased number of particles (Table 4). In this setup, we can observe that the IWAE model performance worsens in terms of held-out likelihood with high number of particles, underlining a well-known behavior of this model [19]. Conversely, increasing the number of particles is more beneficial to WW than to IWAE. WW learns the best generative model (in terms of held-out likelihood) and reaches lower mean absolute errors than IWAE. Intriguing, the performance of the χ -VAE drops significantly on all metrics in this setup. Like in the other experiments, our three-step approach minimizes the MAE, among all generative models/variational distributions pairings (Figure 6).

Table 4: Results on the pPCA simulated data. MAE refers to the mean absolute error in posterior expectation estimation.

	VAE	IWAE	WW	χ -VAE
$\log p_\theta(X)$	-17.22	-16.93	-16.92	-17.28
IWELBO	-17.22	-16.93	-16.92	-17.29
$\ A\ _2$	1.62	0.96	1.16	1.00
PSIS	0.56	0.07	0.49	0.98
MAE	0.062	0.028	0.021	0.073

E.6 Benchmarking for posterior collapse methods

Posterior collapse is an established issue of VAE training, in which the variational network does not depend on the data instance. Currently, two different explanations offer to explain this behavior. In some research lines, it is assumed to be a specificity of the inference procedure[46, 47]. In others, it is supposed to be caused by a deficient model [57]. This last interpretation is beyond the scope of our manuscript. To measure the impact of posterior collapse, we included cyclic KL annealing [46] and lagging inference network [47] baselines to the pPCA experiment. We also considered constant KL annealing, which did not improve performance over cyclical annealing.

Those methods improve the held-out log-likelihood and MAE for the VAE baseline (Table 5), hinting that posterior collapse alleviation can improve decision. However, even the best performing method (lagging inference networks) shows slight improvement compared to the VAE baseline (2% in terms of held-out likelihood) and does not reach the other baselines’ performance. We leave extended studies of posterior collapse effects to future work.

Table 5: Extended results on the pPCA simulated data.

	VAE	AGG	CYCLIC	IWAE	WW	χ -VAE
$\log p_\theta(X)$	-17.65	-17.13	-17.20	-16.91	-16.93	-16.92
IWELBO	-17.66	-17.14	-17.20	-16.92	-16.96	-16.92
$\ A\ _2$	1.69	1.47	1.68	1.30	2.32	1.13
PSIS	0.54	0.55	0.58	0.53	0.66	0.47
MAE	1.03	0.057	0.050	0.032	0.043	0.030

F Supplemental information for the MNIST experiment

F.1 Dataset

We used the MNIST dataset [34], split following a 50% train - 50% test ratio.

F.2 Model details and neural networks architecture

For efficiency considerations, the variational distribution parameters of $q_\phi(z | x)$ were parameterized by a small convolutional neural network (3 layers of kernels of size 3), followed by two fully-connected layers. The parameters of the distributions $q_\phi(c | z), q_\phi(u | z, c), p_\theta(x | z), p_\theta(z | c, u), p_\theta(c)p_\theta(u)$ were all encoded by fully-connected neural networks (one hidden layer of size 128). We used SELU non-linearities [58], and dropout (rate 0.1) between all hidden layers.

All models were trained for 100 epochs using the Adam optimizer (learning rate of 0.001, batch size 512).

F.3 Additional results

All models show relatively similar accuracy levels (Figure 7). The three-step procedure applied to the best generative model (IWAE) provides the best levels of accuracy.

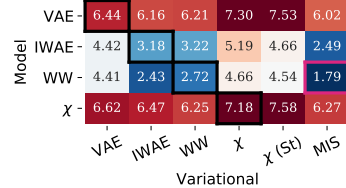


Figure 6: MAE ($\times 10^2$) for pPCA: combinations of VAEs (row) and inference only (columns) frameworks.

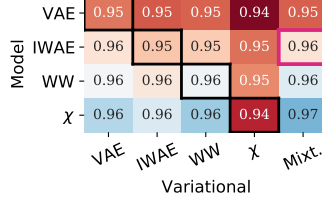


Figure 7: Accuracy for M1+M2: combinations of VAEs (row) and inference only (columns) frameworks.

F.4 Estimation of posterior expectations for the M1+M2 model

We derive here the two estimators for estimating $p_\theta(c | x)$ in the M1+M2 model. First, we remind the reader that the generative model is

$$p_\theta(x, z, c, u) = p_\theta(x | z)p_\theta(z | c, u)p_\theta(c)p_\theta(u), \quad (67)$$

and that the variational distribution factorizes as

$$q_\phi(z, c, u | x) = q_\phi(z | x)q_\phi(c | z)q_\phi(u | z, c). \quad (68)$$

Plugin approach For the plugin approach, we compute $q_\phi(c | x)$ as:

$$q_\phi(c | x) = \iint_{z,u} q_\phi(c, u, z | x) dudz \quad (69)$$

$$= \iint_{z,u} q_\phi(u | c, z)q_\phi(c, z | x) dudz \quad (70)$$

$$= \iint_z q_\phi(c | z)q_\phi(z | x) dz, \quad (71)$$

where the last integral is estimated with naive Monte Carlo.

SNIS approach We obtain $p_\theta(c, x)$ via marginalization of the latent variables z, u :

$$p_\theta(c, x) = \iint p_\theta(x, u, c, z) dz du. \quad (72)$$

We may estimate this probability, for a fixed c , using $q_\phi(z, u | x, c)$ as a proposal for importance sampling:

$$p_\theta(c, x) = \mathbb{E}_{q_\phi(z, u | x, c)} \left[\frac{p_\theta(x, u, c, z)}{q_\phi(z, u | x, c)} \right]. \quad (73)$$

Then, the estimates for $p_\theta(c, x)$ may be normalized by their sum for all labels (equals to $p_\theta(x)$) to recover $p_\theta(c | x)$.

Interestingly, this estimator does not make use of the classifier $q_\phi(c | z)$, so we expect it to have a possibly lower performance than the plugin. Indeed, the $q_\phi(c | z)$ is fit with a classification loss towards the labelled datapoints.

G Analysis of alternate divergences for the M1+M2 model

We have the following pathological behavior, similar to the one presented in the factor analysis instance. This ill-behavior is further exacerbated when the M1+M2 model is fitted with a composite loss as in Equation 9 of [35]. Indeed, neural networks are known to have poorly calibrated uncertainties [59].

Proposition 2. *Consider the model defined in Eq. (10). Assume that posterior inference is exact for latent variables u and z , such that $q_\phi(z | x)q_\phi(u | c, z) = p_\theta(z, u | c, x)$. Further, assume that for a fixed $z \in \mathcal{Z}$, $p_\theta(c | z)$ has complete support. Then, as $\mathbb{E}_{q_\phi(c | z)} \log q_\phi(c | z) \rightarrow 0$, it follows that*

1. $\Delta_{KL}(q_\phi(c, z, u | x) \| p_\theta(c, z, u | x))$ is bounded;

2. $\Delta_{KL}(p_\theta(c, z, u | x) \| q_\phi(c, z, u | x))$ diverges; and
3. $\Delta_{\chi^2}(p_\theta(c, z, u | x) \| q_\phi(c, z, u | x))$ diverges.

Proof. The proof mainly consists in decomposing the divergences. The posterior for unlabelled samples factorizes as

$$p_\theta(c, u, z | x) = p_\theta(c | z)p_\theta(z, u | x, c). \quad (74)$$

From this, expression of the other divergences follow under the semi-exact inference hypothesis. Remarkably, all three divergences can be decomposed in similar forms. Also, the expression of the divergences can be written in closed form (recall that c is discrete) and as a function of λ .

Reverse-KL. In this case, the Kullback-Leibler divergence can be written as

$$\Delta_{KL}(q_\phi(c, z, u | x) \| p_\theta(c, z, u | x)) = \mathbb{E}_{q_\phi(c|z)} \Delta_{KL}(q_\phi(z, u | x, c) \| p_\theta(z, u | x, c)) \quad (75)$$

$$+ \mathbb{E}_{q_\phi(z|x)} \Delta_{KL}(q_\phi(c | z) \| p_\theta(c | z)), \quad (76)$$

which further simplifies to

$$\Delta_{KL}(q_\phi(c, z, u | x) \| p_\theta(c, z, u | x)) = \mathbb{E}_{p_\theta(z|x)} \Delta_{KL}(q_\phi(c | z) \| p_\theta(c | z)).$$

This last equation can be rewritten as a constant plus the differential entropy of $q_\phi(c | z)$, which is bounded by $\log C$ in absolute value.

Forward-KL. Similarly, we have that

$$\begin{aligned} \Delta_{KL}(p_\theta(c, z, u | x) \| q_\phi(c, z, u | x)) &= \mathbb{E}_{p_\theta(c|z)} \Delta_{KL}(p_\theta(z, u | x, c) \| q_\phi(z, u | x, c)) \\ &+ \mathbb{E}_{p_\theta(z|x)} \Delta_{KL}(p_\theta(c | z) \| q_\phi(c | z)), \end{aligned}$$

which also further simplifies to

$$\begin{aligned} \Delta_{KL}(p_\theta(c, z, u | x) \| q_\phi(c, z, u | x)) &= \mathbb{E}_{p_\theta(z|x)} \Delta_{KL}(p_\theta(c | z) \| q_\phi(c | z)) \\ &= \mathbb{E}_{p_\theta(z|x)} \sum_{c=1}^C p_\theta(c | z) \log \frac{p_\theta(c | z)}{q_\phi(c | z)}. \end{aligned}$$

This last equation includes terms in $p_\theta(c | z) \log q_\phi(c | z)$, which are unbounded whenever $q_\phi(c | z)$ is zero but $p_\theta(c | z)$ is not.

Chi-square. Finally, for this divergence, we have the decomposition

$$\Delta_{\chi^2}(p_\theta(c, z, u | x) \| q_\phi(c, z, u | x)) = \mathbb{E}_{q_\phi(z, c, u | x)} \frac{p_\theta^2(z, u | x, c)p_\theta^2(c | z)}{q_\phi^2(z, u | x, c)q_\phi^2(c | z)},$$

which in that case simplifies to

$$\Delta_{\chi^2}(p_\theta(c, z, u | x) \| q_\phi(c, z, u | x)) = \mathbb{E}_{p_\theta(z|x)} \Delta_{\chi^2}(p_\theta(c | z) \| q_\phi(c | z)).$$

Similarly, the last equation includes terms in $p_\theta^2(c | z) / q_\phi(c | z)$, which are unbounded whenever $q_\phi(c | z)$ is zero but $p_\theta(c | z)$ is not. \square

H Supplemental information for the single-cell experiment

H.1 Dataset

Let N, G , respectively denoting the number of cells and genes of the dataset. We simulated scRNA counts from two cell-states a, b , each following Poisson-LogNormal distributions of respective means $\mu_{ag}, \mu_{bg}, g \leq G$ and sharing covariance Σ . For each cell n , the cell-state c_n is modelled as a categorical distribution of parameter p . The underlying means follow Lognormal distributions

$$h_{ng} \sim \text{Lognormal}(\mu_{c_n}, \Sigma).$$

Counts x_{ng} for cell n and gene g are assumed to have Poisson noise

$$x_{ng} \sim \text{Poisson}(h_{ng}).$$

We now clarify how the Lognormal parameters were constructed. Both populations shared the same covariance structure

$$\Sigma = (0.5 + u)I_g + 2aa^T, \text{ where } \begin{cases} a \sim \mathcal{U}((-1, 1)^g) \\ u \sim \mathcal{U}((-0.25, 0.25)^g). \end{cases}$$

The ground-truth LFC values Δ_g between the two cell states, a and b , were randomly sampled in the following fashion. We first randomly assign a differential expression status to each gene. It can correspond to similar expression, up-regulation, or down-regulation between the two states for the gene. Conditioned to this status, the LFCs were drawn from Gaussian distributions respectively centered on 0, -1 , and 1 and of standard deviation $\sigma = 0.16$.

Finally, gene expression means for population a were sampled uniformly on $(10, 100)$ populations b obtained as

$$\mu_b = 2^{\Delta_g} \mu_a.$$

In our experiments, we used $N = 1000$, $G = 100$, and followed a 80% – 20% train-test split ratio.

H.2 Model details and neural networks architecture

We introduce here a variant of scVI as a generative model of cellular expression counts. For more information about scVI, please refer to the original publication [7].

Brief background on scVI Latent variable $z_n \sim \text{Normal}(0, I_d)$ represents the biological state of cell n . Latent variable $l_n \sim \text{LogNormal}(\mu_l, \sigma_l^2)$ represents the library size (a technical factor account for sampling noise in scRNA-seq experiments). Let f_w be a neural network. For each gene g , expression count x_{ng} follows a zero-inflated negative binomial distribution, whose negative binomial mean is the product of the library size l_n and normalized mean $h_{ng} = f_w(z_n)$. The normalized mean h_{ng} is therefore deterministic conditional on z_n ; it will have the uncertainty in the posterior due to z_n . The measure $p_\theta(h_{ng} | x_n)$ denotes the push-forward of $p_\theta(z_n | x_n)$ through the g -th output neuron of neural net f_w . scVI therefore models the distribution $p_\theta(x)$.

Differences introduced In our experiments, the importance sampling weights for all inference mechanisms had high values of PSIS diagnostic for the original scVI model. Although the FDR control was more efficient with alternative divergences, our proposal distributions were poor. The posterior variance for latent variable l_n could reach high values, leading to numerical instabilities for the importance sampling weights (at least on this dataset). To work around the problem, we removed the prior on l_n and learned a generative model for the conditional distribution $p_\theta(x_n | l_n)$ using the number of transcripts in cell n as a point estimate of l_n .

H.3 Additional results

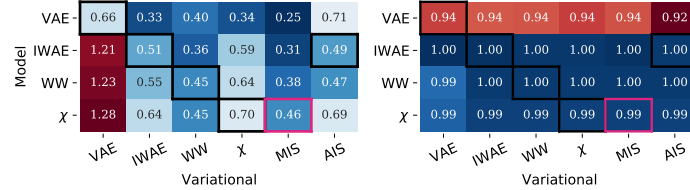


Figure 8: PSIS (left) and PRAUC (right) for scVI: combinations of VAEs (row) and inference only (columns) frameworks.

We emphasize that the PSIS metric does not provide a full picture to select a decent model/variational distribution combination. On the differential expression task, most combinations using the VAE as generative models offer appealing PSIS values (Figure 8). However, these combinations offer deceiving gene rankings, as hinted by their PRAUC ($AUC = 0.94$). Besides, the variational distributions trained using the classical ELBO used in combination with IWAE, WW, or χ are inadequate for decision-making. These blends reach inadmissible levels of PSIS.

To assess the different models potential for differential expression, we compare the FDR evolution with the posterior expected FDR of the gene rankings obtained by each model (Figure 9). The match between these quantities for IWAE and χ hints that they constitute sturdy approaches for differential expression tasks, while the traditional VAE fails to estimate FDR reliably.

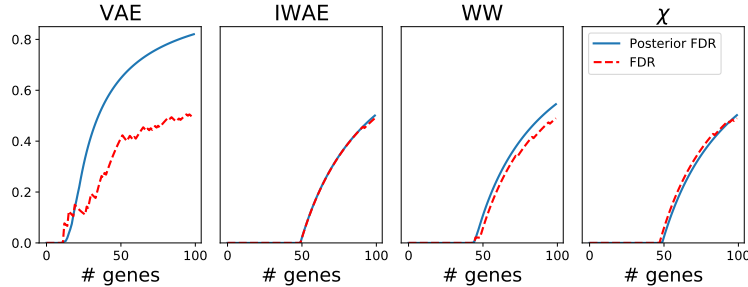


Figure 9: Posterior expected FDR (blue) and ground-truth FDR (red) of the decision rules consisting in selecting the genes with the highest DE probability for the different models.